Microwave Imaging Based on Compressed Sensing Using Adaptive Thresholding

Masoumeh Azghani[1], Panagiotis Kosmas[2], Farokh Marvasti[1]
[1]Advanced Communications Research Institute (ACRI), Sharif University of Technology, Iran
[2]School of Natural and Mathematical Sciences, King's College London, London, WC2R 2LS, U.K.

***Abstract*—We propose to use a compressed sensing recovery method called IMATCS for improving the resolution in microwave imaging applications. The electromagnetic inverse scattering problem is solved using the Distorted Born Iterative Method combined with the IMATCS algorithm. This method manages to recover small targets in cases where traditional DBIM approaches fail. Furthermore, by applying an L_2-based approach to regularize the sparse recovery algorithm, we improve the algorithm's robustness and demonstrate its ability to image complex breast structures. Although our simulation scenarios do not fully represent experimental or clinical data, our results suggest that the proposed algorithm may be able to overcome persistent challenges in microwave medical imaging.**

***Index Terms*—Microwave tomography, compressed sensing, adaptive thresholding, breast imaging, inverse scattering**

I. Introduction

Microwave tomographic methods for clinical applications estimate the spatial distribution of dielectric properties in a tissue region by solving an electromagnetic (EM) inverse scattering problem [1]- [3]. In this paper, microwave tomography is implemented by applying the Distorted Born Iterative Method (DBIM) which, as any GN approach, approximates the non-linear inverse scattering problem with an underdetermined set of linear equations.

We propose a novel solution to the resulting linear system based on an Iterative Method with Adaptive Thresholding for Compressed Sensing (IMATCS) [4], [5], which is a variant of the so-called Iterative Hard Thresholding (IHT) method [6]. The main advantage of the IMATCS method over IHT is that it does not require the sparsity dimension of the signal as a prior knowledge for signal recovery. We also propose a novel L_2-regularized version of IMATCS, which is tested in scenarios where the original IMATCS becomes unstable. The proposed approach belongs to a wider category of sparsity regularization techniques, which are currently pursued in microwave imaging (MWI). In [7], for example, an L_1 regularizer is exploited to encourage sparsity in contrast-enhanced MWI of breast tumors. The elastic net method is proposed in [8] to solve the linear problem within the DBIM, resulting in an improvement in reconstructions of the breast interior.

To demonstrate that the proposed method can achieve super-resolution in microwave imaging, we have considered simplified homogeneous breast models with closely located tumor-like scaterrers of various size. We have also tested the ability of the regularized version of our algorithm to image complex breast structures by considering a highly heterogenous breast distribution. Although our simulation scenarios are simplified and do not correspond to clinical data, they are very useful in demonstrating the advantages of the proposed approach over other existing MWI algorithms. The rest of the paper is organized as follows: Section II reviews EM inverse scattering within the DBIM and introduces the IMATCS approach. Simulation results are presented in Section III, while Section IV concludes the paper with some additional comments.

II. Methods

The DBIM algorithm is based on the distorted-wave Born integral equation,

$$\mathbf{E}^{sc}(\mathbf{r}) = \mathbf{E}^{t}(\mathbf{r}) - \mathbf{E}^{b}(\mathbf{r}) = \omega^2\mu \int_V d\mathbf{r}' \bar{\mathbf{G}}^{b}(\mathbf{r},\mathbf{r}')\Delta\epsilon(\mathbf{r}')\mathbf{E}^{b}(\mathbf{r}') \tag{1}$$

where $\mathbf{E}^{sc}$ is the scattered electric field, $\Delta\epsilon(\mathbf{r}') = \epsilon(\mathbf{r}') - \epsilon_b(\mathbf{r}')$ is the unknown contrast function over the volume of support V, and $\bar{\mathbf{G}}^{b}(\mathbf{r},\mathbf{r}')$ denotes the dyadic background Green's function, which represents propagation from the source located at $\mathbf{r}$ to the point $\mathbf{r}'$ inside V. The (unknown) total field $\mathbf{E}^{t}$ is approximated with the (known) background field $\mathbf{E}^{b}$ inside the integral in (1). The resulting linear integral equation is solved in the discrete domain at each iteration of the DBIM algorithm for the contrast function $\Delta\epsilon(\mathbf{r}')$.

Based on the above, we can express the linear problem et each DBIM iteration in (1) as,

$$y = \Phi x \tag{2}$$

where Φ is an $M \times N$ measurement matrix ($M < N$) and x represents the N-dimensional signal of interest. We wish to recover the unknown signal from the measurement vector y, given that the number of measurements M is much lower than the number of signal entries N. Compressed sensing (CS) theory solves this underdetermined problem by assuming that the signal is sparse [9].

Among various CS approaches, the IMATCS method is based on the IHT method, which solves the following optimization problem,

$$\min_{\mathbf{x}} \|\mathbf{y} - \mathbf{\Phi x}\|_2^2 + \lambda\|\mathbf{x}\|_0 \tag{3}$$

The solution of (3) can be written as,

$$x_{k+1} = H(x_k + \Phi^T(y - \Phi x_k)) \tag{4}$$

978-88-907018-4-9/14/$31.00 ©2014 IEEE

where $H(z)$ is the hard thresholding function which discards all but K absolutely maximum entries of z. The sparsity number K of the signal is required to be known *a priori* to recover the underlying signal. However, it is usually impossible to know the proper value of K before recovering it. In order to get around this problem, IMATCS takes advantage of an adaptive thresholding procedure. The mathematical formulation of the method rewrites (4) as,

$$x_{k+1} = H(x_k + \lambda \Phi^T (y - \Phi x_k)) \tag{5}$$

where λ is the relaxation parameter which controls the convergence of the algorithm and H is the thresholding function, which is decreased in an exponential manner as $T = T_0 e^{-\alpha i}$, where i is the iteration number, T_0 is the initial threshold value and α indicates the threshold step. The algorithm starts from zero initial value, $x_0 = 0$. The coefficient vector is recovered as $x_{maxiter}$, after a "$maxiter$" number of iterations. The adaptivity of the threshold enables us to recover the embedding signal from its linear measurements without any knowledge of the sparsity number of the signal.

To deal with the ill-posedness of the EM inverse scattering problem, we have implemented an L_2-regularized variant of the IMATCS algorithm, which solves the minimization problem,

$$\min_{\mathbf{x}} \|\mathbf{y} - \mathbf{\Phi x}\|_2^2 + \lambda_1 \|\mathbf{x}\|_1 + \lambda_2 \|\mathbf{x}\|_2^2 \tag{6}$$

The above cost function is similar to the elastic net approach in [8]. However, the L_2-IHT method is much simpler than the elastic net approach, and thus leads to an algorithm which is orders of magnitude faster. Based on (6), the $L_1 - L_2$ regularized problem is solved by modifying (5) as,

$$x_{k+1} = \frac{1}{1+\lambda_2} H(x_k + \lambda_1 \Phi^T (y - \Phi x_k)) \tag{7}$$

The introduction of the Tikhonov parameter λ_2 controls the stability of the algorithm by promoting L_2-based solutions of the minimization problem in (6). Thus, the overall performance of the proposed L_2-IMATCS method is determined by the choice of the regularization parameters λ_1 and λ_2, and the thresholding function parameters T_0, α, and "$maxiter$". In the simulations of the next section, we have set λ_1 as,

$$\lambda_1 = \frac{1.9}{\max eig(\Phi^H \Phi)} \tag{8}$$

where *eig* denotes matrix eigenvalues, and Φ is the measurement matrix in (2), which is updated at each DBIM iteration.

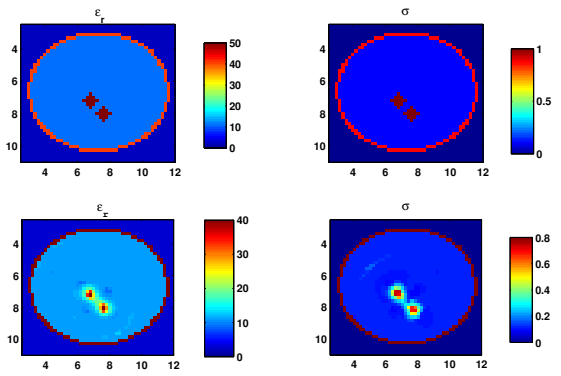

Fig. 1. Dielectric constant ϵ_r and conductivity σ distributions at 1 GHz of a 2-D homogeneous breast phantom with two small tumors. The top plots represent the true ϵ_r and σ values and the bottom plots the values estimated by the L2-IMATCS algorithm for $\lambda_2 = 0.005$.

III. Results

Our simulations are based on the finite-difference-time-domain (FDTD) method with a uniform grid cell size of 2.0 mm to simulate measured data, which is also used for the inversion process. This "inverse crime" assumption allows us to benchmark the performance of our approach. The algorithm estimates the parameters ϵ_∞, ϵ_s, and σ_s of the Debye model for the complex relative permittivity, $\epsilon_r(\omega) = \epsilon_\infty + \frac{\epsilon_s - \epsilon_\infty}{1+j\omega\tau} - j\frac{\sigma_s}{\omega\epsilon_0}$. As in previous work [3], τ is assumed constant for all tissues (with a value of 17.1 ps). Dipole antennas (which correspond to point sources for the 2-D simulations) illuminate the breast with a wideband pulse sequentially, and also record the data to be used for the solution of the microwave tomographic problem. The background medium is assumed lossless with $\epsilon_r = 2.6$, and the Debye parameters for the various tissues are extracted from UW-Madison's repository data [10].

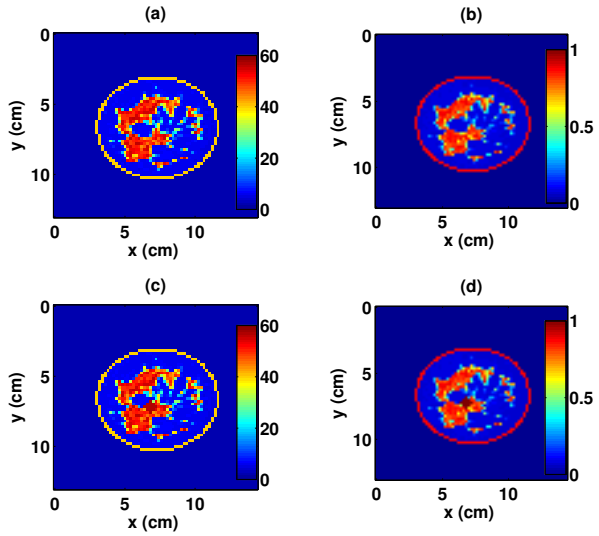

Fig. 2. (a), (c) Dielectric constant ϵ_r and (b), (d) conductivity σ distributions at 1 GHz of the 2-D axial slice taken from a heterogenously dense breast phantom [10], which is used as testbed for the proposed algorithm. A tumor is included in the bottom images.

We first consider two closely located tumor-like scatterers in a simplified breast model, which represents cases where the dielectric distribution is sparse in the reconstruction domain. The true and estimated dielectric contrast and conductivity distributions calculated at 1GHz for this simulation scenario are shown in Fig. 1. It is clear from the figure that the IMATCS-DBIM algorithm manages to reconstruct both tumors, while traditional L_2-based algorithms result in a blurred

image of only one scatterer. This result demonstrates the super-resolution properties of the proposed algorithm.

Next, we demonstrate the robustness of our regularized IMATCS-DBIM algorithm in reconstructing complex breast structures. To this end, we have applied the previous setup to a 2-D coronal slice from a "heterogeneous breast" phantom taken from UW-Madison's online breast phantom repository [10]. The dielectric constant and conductivity distributions of the considered coronal slice are shown in Fig. 2. Fig. 3 presents reconstructions of the dielectric constant and conductivity distributions for the breast phantom depicted in Fig. 2, with and without a tumor. These images are obtained by the regularized IMATCS-DBIM algorithm using data from six equally spaced frequencies in the range $1.2-2.7$ GHz, after an initial estimate at 1 GHz is obtained. While *a priori* knowledge of the skin properties was assumed in these reconstructions as in previous work [3], we have obtained images of similar quality without any prior knowledge of the skin layer. We note that conventional CGLS or LSQR algorithms fail to reconstruct the breast structure in these cases.

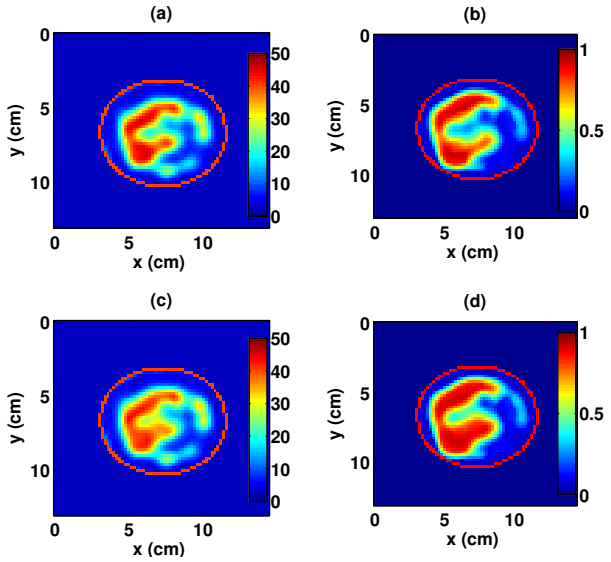

Fig. 3. (a), (c) Dielectric constant ϵ_r and (b), (d) conductivity σ estimated distributions at 1 GHz of the 2-D breast phantom in Fig. 2. Small differences in the neighborhood of the tumor are observed in the these images.

IV. Conclusion

We have proposed a novel MWI algorithm based on the DBIM approach and the IMATCS algorithm. Our initial simulations have demonstrated the advantages and potential of this method for super-resolution microwave breast imaging. Our future work will focus on examining this approach further by expanding it for three-dimensional configurations and testing it with experimental data.

References

[1] S. Semenov, "Microwave tomography: Review of the progress towards clinical applications," *Phil. Trans. R. Soc. A*, vol. 367, pp. 3021-3042, 2009.

[2] P. M. Meaney, M. W. Fanning, T. Raynolds, C. J. Fox, Q. Q. Fang, C. A. Kogel, S. P. Poplack, and K. D. Paulsen, "Initial clinical experience with microwave breast imaging in women with normal mammography," *Acad. Radiol.*, vol. 14, no. 2, pp. 207-218, Feb. 2007.

[3] J. D. Shea, P. Kosmas, S. C. Hagness, and B. D. Van Veen, "Three-dimensional microwave imaging of realistic numerical breast phantoms via a multiple-frequency inverse scattering technique," *Med. Phys.*, vol. 37, no. 8, pp. 4210-4226, Aug. 2010.

[4] M. Azghani and F. Marvasti, "Iterative algorithms for random sampling and compressed sensing recovery," *in Internat. Workshop Sampling Theory and Applications*, Bremen, Germany, July 2013.

[5] F. Marvasti, A. Amini, F. Haddadi, M. Soltanolkotabi, B. H. Khalaj, A. Aldroubi, S. Holm, S. Sanei, and J. Chambers, "A unified approach to sparse signal processing," *EURASIP Journal on Advances in Signal Processing*, 2012.

[6] T. Blumensath and M. E. Davies, "Iterative hard thresholding for compressed sensing," *App. Computat. Harm. Analysis*, vol. 27, no. 3, pp. 265-274, 2009.

[7] F. Gao, B. Veen, and S. Hagness, "Contrast enhanced microwave imaging of breast tumors using sparsity regularization," *in Proc. 2012 IEEE Antennas Propagat. Soc. Internat. Symp. (APS-URSI)*, pp.8-14, Chicago, IL, July 2012.

[8] D. Winters, B. Veen, and S. Hagness, "A sparsity regularization approach to the electromagnetic inverse scattering problem," *IEEE Trans. Antennas Propagat.*, vol. 58, no. 1, pp. 145154, Jan. 2012.

[9] E. Candes and M. B. Wakin, "An introduction to compressive sampling," *IEEE Signal Processing Magazine*, vol. 25, no. 2, pp. 2130, Mar. 2008.

[10] E. Zastrow, S. K. Davis, M. Lazebnik, F. Kelcz, B. D. Van Veen, and S. C. Hagness, "Development of anatomically realistic numerical breast phantoms with accurate dielectric properties for modeling microwave interactions with the human breast," *IEEE Trans. Biomed. Eng.*, vol. 55, no. 12, pp. 2792-2800, Dec. 2008 [Database available online: http://uwcem.ece.wisc.edu/].